JOURNAL OF GEOPHYSICAL RESEARCH, VOL. 114, D11112, doi:10.1029/2008JD010475, 2009

Tropical Pacific–high latitude south Atlantic teleconnections as seen in $\delta^{18}O$ variability in Antarctic coastal ice cores

D. V. Divine,[1] E. Isaksson,[1] M. Kaczmarska,[1] F. Godtliebsen,[2] H. Oerter,[3] E. Schlosser,[4] S. J. Johnsen,[5] M. van den Broeke,[6] and R. S. W. van de Wal[6]

Received 22 May 2008; revised 4 April 2009; accepted 16 April 2009; published 9 June 2009.

[1] We use a network of eight ice cores from coastal Dronning Maud Land (DML), Antarctica, to examine the role of the tropical ENSO (El Niño-Southern Oscillation) in the temporal variability of $\delta^{18}O$ in annual accumulation. The longest record from the S100 ice core covering the period 1737–1999 is used to analyze the teleconnections between the tropical Pacific and coastal DML on decadal scales and longer. A shorter stacked coastal DML $\delta^{18}O$ series spanning 1955–1999 is constructed to assess the variability of ENSO teleconnection on interannual scales. Results suggest that, on typical ENSO timescales of 2–6 years, the strength of the teleconnection varies in time, being stronger for years with generally negative phase of the Southern Annular Mode (SAM). On the timescales of approximately two decades (bidecadal), positive isotope anomalies are associated with oceanic warming and a westward sea surface temperature (SST) gradient in the equatorial Pacific. Bidecadal variability in SAM, forced by the tropical Pacific, is proposed as a critical element in the teleconnection. Our analysis suggests that a multidecadal positive trend in the annual mean $\delta^{18}O$ values from the analyzed cores can be indicative of the atmospheric warming that begun in this part of the DML already in the 1910s. The trend in $\delta^{18}O$, quantified in terms of long-term surface air temperature (SAT) changes, is consistent with the instrumental data. Yet, we speculate that the accurate estimation of SAT trends requires an assessment of the potential role of secular SAM and sea ice extent changes in shaping the isotopic signal.

Citation: Divine, D. V., E. Isaksson, M. Kaczmarska, F. Godtliebsen, H. Oerter, E. Schlosser, S. J. Johnsen, M. van den Broeke, and R. S. W. van de Wal (2009), Tropical Pacific–high latitude south Atlantic teleconnections as seen in $\delta^{18}O$ variability in Antarctic coastal ice cores, *J. Geophys. Res.*, *114*, D11112, doi:10.1029/2008JD010475.

1. Introduction

[2] There is still much unknown about the recent climate of the Antarctic continent partly due to the limitations in spatial and temporal coverage of instrumental records [e.g., *Turner et al.*, 2005]. While warming of the Antarctic Peninsula region [*King and Harangozo*, 1998] and the possible effects on the local ice shelves breakup [*Vaughan and Doake*, 1996] have received much attention during the last decades, such changes appear not to be evident on the Antarctic continent. The instrumental records from across the Antarctic show no evidence of a geographically wide warming trend of surface temperature over the continent during the last 40–50 years [*Turner et al.*, 2005]. There are individual records that show a statistically significant trend with either warming (such as Novolazarevskaya) or cooling (such as South Pole), but most records are too short to be used for any conclusive trend analyses [*Turner et al.*, 2005]. The warming over the Antarctic Peninsula region is likely a part of a warming that started about a century ago, as suggested by the early expedition records from Antarctica [*Jones*, 1990].

[3] An important climatic parameter is the sea ice surrounding the Antarctic continent. Since the satellite monitoring of sea ice started in 1973, no clear trends have been observed, other than a rather complicated pattern around the continent [e.g., *Parkinson*, 2004]. The period, for which both sea ice extent variability data recorded from satellites and instrumental air temperature records are available, is relatively short, and the connection between them is not easy to interpret [*Turner et al.*, 2005]. However, the long-term monitoring of sea ice conditions from the South Orkney Islands has shown a decrease in sea ice duration since 1903 [*Murphy et al.*, 1995]. This is in agreement with the air temperature series during this period measured at Orcadas meteorological station.

[1]Norwegian Polar Institute, Tromsø, Norway.
[2]Department of Mathematics and Statistics, University of Tromsø, Tromsø, Norway.
[3]Alfred Wegener Institute for Polar and Marine Research, Bremerhaven, Germany.
[4]Institute of Meteorology and Geophysics, University of Innsbruck, Innsbruck, Austria.
[5]Centre for Ice and Climate, Niels Bohr Institute, University of Copenhagen, Copenhagen, Denmark.
[6]Institute for Marine and Atmospheric Research, Utrecht University, Utrecht, Netherlands.

0148-0227/09/2008JD010475$09.00

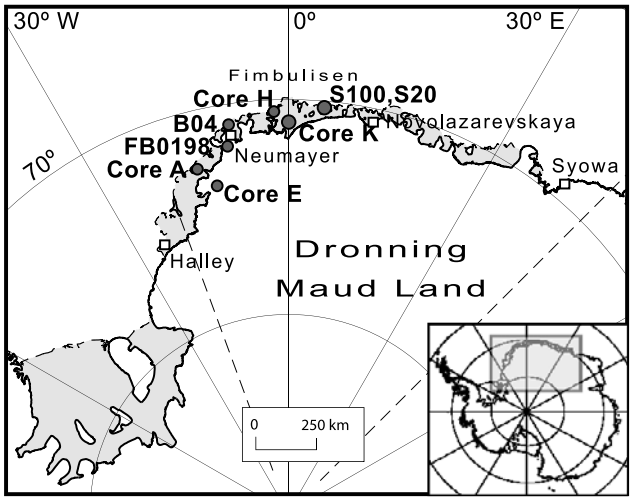

Figure 1. Map of Dronning Maud Land (DML). Location in Antarctica is shown in the insert map (gray square). Stations (open squares) and ice core locations (open circles). For coordinates of the drilling sites, see Table 1.

[4] In recent years there has been increased focus on the interaction between Antarctic climate and ENSO [e.g., *Gregory and Noone*, 2008; *Turner*, 2004; *White and Peterson*, 1996; *Yuan*, 2004]. Since the most pronounced ENSO teleconnections are found over the southeast Pacific, it is expected that, in Antarctica, the strongest ENSO signal should be observed in the Amundsen-Bellingshausen Sea sector. However, the Atlantic sector, and thus our study area, is directly coupled to the Pacific by the Southern Annular Mode, which basically expresses the meridional pressure gradient between the sub-Antarctic and midlatitudes. This pressure gradient determines the strength and meridionality/zonality of the circumpolar band of westerlies and thus the meridional heat and vapor exchange between Antarctica and its surroundings.

[5] The coupled atmosphere-ocean-sea ice system is highly nonlinear with different response times of all single components. This leads to time lags within the system and between ENSO and Antarctic signals, which hamper the progress of understanding the ongoing processes. Ice core records, in particular the water isotope records, which can provide insight on past local surface air temperature (SAT) changes, are important tools when trying to extend the instrumental records further back in time. Through the European Project for Ice Coring in Antarctica (EPICA), Dronning Maud Land has been intensively investigated during the past decade. The major focus has been on long-term climate variability [e.g., *EPICA Community Members*, 2006]. As a part of the EPICA presite survey, one 100 m deep ice core (S100) was drilled on the Fimbulisen ice shelf at 60 m a.s.l. during the Norwegian Antarctic Research Expedition (NARE) in 2000/01 (Figure 1 [*Kaczmarska et al.*, 2004, 2006]). Relatively few coastal ice cores have been drilled around the Antarctic continent and one of the aims of the study with core S100 is to improve the spatial coverage, and evaluate the results in relation to data from the polar plateau.

[6] In this paper we discuss what could influence the variability of the oxygen isotope record from this ice core and a number of shallow cores drilled earlier in the area, with a special focus on the possible role of ENSO. Section 2 presents the network of ice cores together with other data and methods used in this work. Section 3.1 discusses the isotopic signals from S100 and other cores in both the time and frequency domains. The effect of teleconnections between the tropical Pacific and coastal DML on δ^{18}O of accumulated snow at different timescales is analyzed in section 3.2. Section 3.3 presents multidecadal trends in δ^{18}O records from the study area quantified in terms of equivalent SAT changes. The results of the work are summarized in section 4.

2. Ice Cores Description, Dating, and Methods

2.1. Field and Laboratory

[7] Figure 1 shows the network of ice cores used in the present study. Table 1 provides details about core locations with an overview of the oxygen isotope data used. All these cores were drilled during the 1980s–1990s in the coastal area of DML. Core E is the only one of these ice cores retrieved from grounded ice at an altitude of 700 m a.s.l. while the others were drilled at coastal sites on ice shelves. All oxygen isotope values were published earlier. A detailed description of each of the time series can be found in the works of *Isaksson and Karlén* [1994] (Core A), *Isaksson et al.* [1996] (Core E), *Melvold* [1999] (Cores H, K), *Isaksson et al.* [1999] (Core S20), *Kaczmarska et al.* [2004, 2006] (S100), and *Schlosser and Oerter* [2002b] (B04, FB0198).

[8] The most recent 100 m long ice core named S100 was retrieved with an electromechanical drill in the eastern part of the Fimbulisen ice shelf (Figure 1) at 70°14′S, 04°48′E; 48 m a.s.l. during NARE 2000/01 [*Kaczmarska et al.*,

Table 1. Ice Cores From the Coastal DML Used in the Present Study

Site	Location	Altitude m a.s.l.	Core Length m	Mean Annual Accumulation m w.e.	Time Coverage (Dating Error) years	Mean δ^{18}O per mille	STD δ^{18}O per mille	10 m Temperature °C
Core A	72°39′S, 16°38′W	60	10.1	0.38	1975–1989 (±1)	−21.2	1.4	−16.7
Core E	73°36′S, 12°26′W	700	30.4	0.32	1932–1991 (±3)	−26.5	1.4	−22.0
Core H	70°30′S, 02°27′W	53	31.9	0.48	1953–1993 (±1)	−22.1	1.1	−18.4
Core K	70°45′S, 00°00′	53	30.3	0.25	1954–1996 (±2)	−22.7	1.5	−19.6
Core B04	70°39′S, 08°15′W	50	52.0	0.35	1892–1981 (±1)	−20.7	1.7	n.a.
Core FB9801	70°71′S, 08°43′W	35	27.8	0.32	1955–1997 (±1)	−20.8	1.5	n.a.
Core S20	70°14′S, 04°48′E	63	20	0.27	1955–1996 (±3)	−20.4	2.4	−17.5
Core S100	70°14′S, 04°48′E	48	100	0.29	1737–1999 (±3)	−23.5	1.5	−17.5

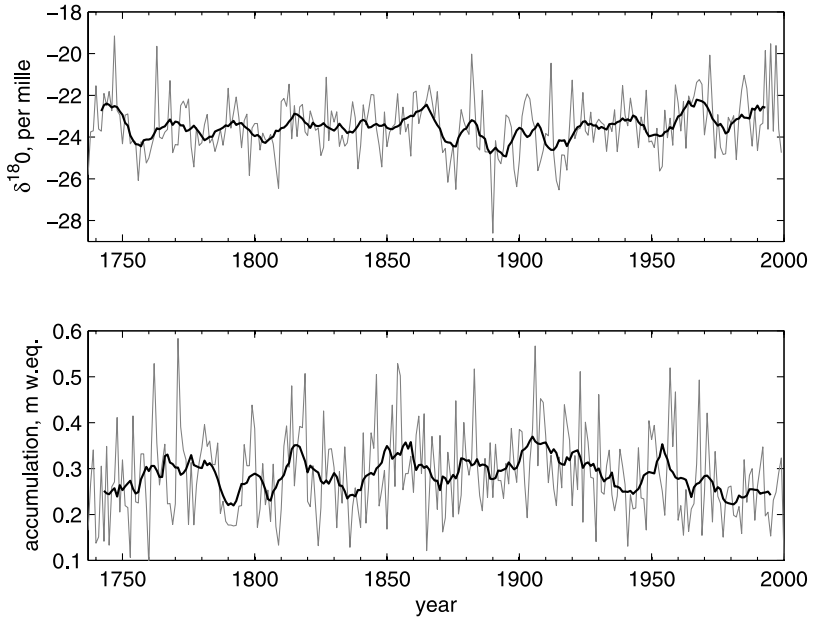

Figure 2. The δ^{18}O and accumulation records from S100 ice core. Gray lines show annual mean values, and the 11-year running means are highlighted in black.

2004]. The 10 m temperature at the drill site was −17.5°C. The ice core has been dated using the combination of electrical conductivity measurements (ECM) and dielectrical profiling (DEP), which helped to identify volcanic eruptions. The obtained age model was cross checked with annual layer count of the seasonally resolved δ^{18}O record. The S100 core covers the period of 1737–2000 A.D. ±3 years [*Kaczmarska et al.*, 2004]. This time series is the longest among the available high-resolution records from this part of coastal DML. For more details about the core and the dating methods we refer to the paper by *Kaczmarska et al.* [2004]. The δ^{18}O sampling was performed in the cold laboratory and samples were taken every 3 cm (equivalent to a minimum of 6 samples/a). The samples were analyzed with the mass spectrometer (VG ISOGAS) at the University of Copenhagen. Since the terrain upstream of the S100 drilling site is basically flat, the lower/older parts of the core originate from areas of only slightly higher altitude, thus no flow correction was applied to the data.

2.2. Data and Procedures

[9] We use two longer series of indices, which capture well the principal features of SST variability in the tropics. The Niño-3.4 index is indicative of coherent SST fluctuations in the entire equatorial Pacific and is generally used as a measure of the amplitude of ENSO. The index is defined as SST averaged over the region of (5°N–5°S, 170–120°W). The second index, introduced by *Trenberth and Stepaniak* [2001] as the difference in normalized anomalies of SST between Niño-1 + 2 (0–10°S, 90–80°W) and Niño-4 (5°N–5°S, 160°E–150°W) regions, gives a measure of the SST gradient across the Pacific basin. The variability associated with TNI index was recently named ENSO Modoki, or pseudo ENSO [*Ashok et al.*, 2007]. We also use the 50-yearlong observation-based Southern Hemisphere Annular Mode Index series (SAM [*Marshall*, 2003]) which provides an indication of the strength of the circumpolar vortex and westerlies that encircle Antarctica.

[10] We have used several different statistical tools in order to detect significant variability on different timescales and infer about the nature of signal captured by δ^{18}O data from the ice cores.

[11] Significant Zero Crossings of Derivatives (SiZer [*Chaudhuri and Marron*, 1999; *Godtliebsen et al.*, 2003]) is a graphical tool used to quantitatively decide which smoothed features are statistically significant at a given threshold. It thus allows us to pick out variations that may be attributable to underlying structure in the data set, as opposed to noise or sampling variability [*Godtliebsen et al.*, 2003]. In SiZer, significant features are found at different scales, e.g., at different levels of data smoothing. Color-coding is used to visualize statistical significance of the data trends at various smoothing timescales. This is controlled by the size of the smoothing window (bandwidth h), and location (x) for the signal. For each scale and location of the signal, SiZer tests whether the smooth has a derivative significantly different from zero.

[12] We use the Multi-Taper Method (MTM) for spectral estimation and reconstruction [*Thomson*, 1982; *Percival and Walden*, 2000]. MTM proved to be a useful tool for exploration of the spectral properties of signals that contain both broadband and oscillatory components. For analysis, we make use of the SSA-MTM toolkit provided by *Ghil et al.* [2002].

[13] For examining relationships between the pairs of time series on different timescales we applied the method of wavelet coherence [*Torrence and Compo*, 1998; *Grinsted et al.*, 2004]. The method shows how coherent two wavelet spectra being analyzed are and can be thought of as a localized correlation coefficient in time frequency space. Following the method proposed in [*Torrence and Compo*, 1998], the wavelet transform is also applied for band-pass

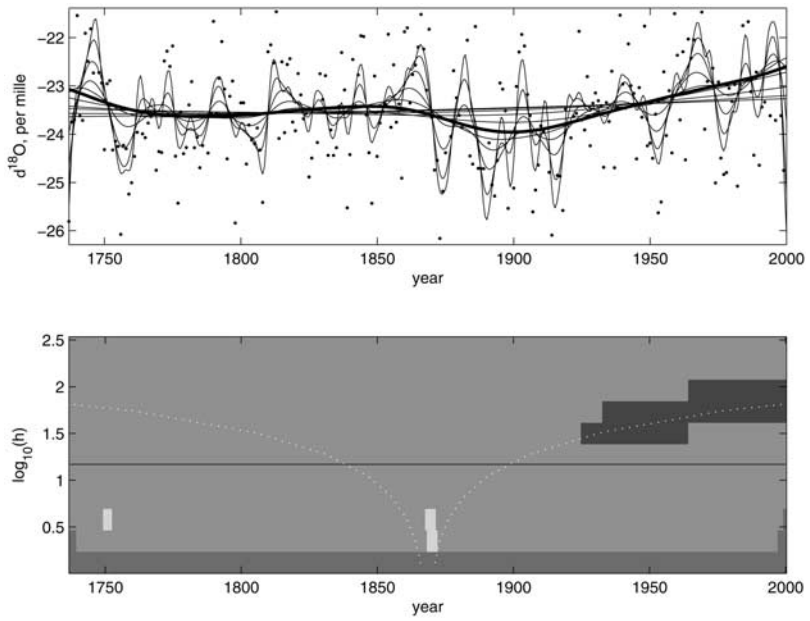

Figure 3. SiZer analysis of the $\delta^{18}O$ record from core S100. (top) Dots, $\delta^{18}O$ samples; lines, family of smoothes obtained for various versions of the bandwidth (h). Thick solid line is for the smooth with $h = \log_{10}(1.2)$ (also marked by a thin horizontal solid line at the bottom). (bottom) SiZer significance test at 95% confidence level. Color coding in SiZer: gray, no significant trend; dark gray, significant increase; light gray, significant decrease. A shaded area at very small scales (below $\log_{10}(0.5)$) is used to indicate that too few data are available to do inference. The interval between two white dotted lines shows the effective width of the smoothing kernel at each h.

filtering of the analyzed records. In both approaches Morlet wavelet is used as a basis function. This wavelet is believed to be an optimal choice providing a good balance between time and frequency localization for features in a spectrum.

3. Results and Discussion

3.1. Oxygen Isotope Records

[14] The annual mean oxygen isotope record from the S100 ice core demonstrates pronounced temporal variations in a range between −29.7‰ and −15.2‰. As mentioned earlier, the $\delta^{18}O$ shows a typical seasonal cyclicity throughout the record [*Kaczmarska et al.*, 2004]. The record shows the most negative mean $\delta^{18}O$ values (i.e., presumably cold periods) occurring during 1870s and 1890s (Figure 2). Periods with the most pronounced positive $\delta^{18}O$ anomalies are centered around 1740, 1865, 1885 and 1965. The 20th century is dominated by a positive trend in the $\delta^{18}O$ values with a magnitude of 0.12 ± 0.05‰ per decade. Analysis with SiZer suggests that the positive trend in $\delta^{18}O$ is statistically significant at 95% confidence level since about 1925 (Figure 3). However, the $\delta^{18}O$ values during the most recent 50-year period do not show, on average, any more positive $\delta^{18}O$ values than the earliest part of the record, i.e., the mid 1700s.

[15] Figure 4 compares the S100 oxygen isotope series with other records from coastal DML. In order to separate intersite variability from the common information shared by the core network, we performed a principal component (PC) analysis on six of eight annual mean $\delta^{18}O$ series available for the period 1955–1991, which is represented in all cores. The two other records were not included in the PC analysis due to their relative shortness (core A) or short time overlap with the other records (B04). The first reconstructed principal component (PC1, blue line in Figure 4) represents some 45% of the total variance in the six records considered. This suggests a predominance of a common process(es) driving the variability of $\delta^{18}O$ in precipitation in the area over the local differences at the core sites. In particular, one should note a tendency to a positive trend in seven of eight records considered, which is, however, statistically significant with the 95% confidence in S20, E, K, B04 and S100 series. A pronounced transition from positive $\delta^{18}O$ anomalies at the end of the 1970s to negative in the early 1980s and positive again in the end of the 1980s is evident in cores S20, K, H, E, A and FB0198. This is also reported by *Schlosser and Oerter* [2002a] (core FB0198) but does not appear in S100. In this core the minimum is observed already at the end of the 1970s, resulting in a relatively poor correspondence with other analyzed records, as indicated by only 7% variance represented by PC1 in S100. It includes $\delta^{18}O$ from the S20 core that was drilled at approximately the same location a few years earlier. We suggest that such a discrepancy could be due to less accurate dating in the upper part of the core, as poor ice quality in the core top prevented carrying out ECM analysis [*Kaczmarska et al.*, 2004].

[16] The recent positive trends in $\delta^{18}O$ appear to be a regional signal [*Isaksson et al.*, 1996; *Isaksson and Melvold*, 2002; *Schlosser and Oerter*, 2002b], but no conclusive reason for this trend has been agreed on. *Isaksson et al.* [1996] and *Isaksson and Melvold* [2002] attributed it to an overall secular warming in the Southern Hemisphere, which is hidden by the shortness of available instrumental records.

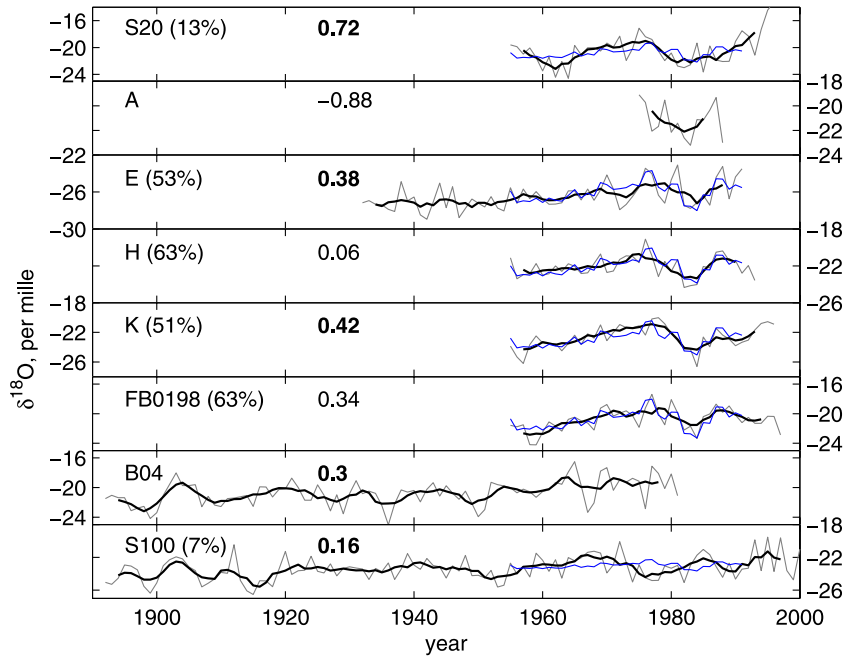

Figure 4. Time series of δ^{18}O from the ice cores used in the study. Gray lines show annual mean values, and the 21-year running means are highlighted in black. Blue lines show the reconstructed PC1 representing some 45% of common variance in δ^{18}O series from S20, E, H, K, FB0198, and S100 during the period 1955–1991. The corresponding amount of variance represented by PC1 in each individual record is indicated in parentheses. Numbers on panels represent the magnitudes of linear trends in δ^{18}O in ‰/decade. Statistically significant at the 95% confidence level values of trends, according to *F* test, are highlighted in bold. Note that for B04 and S100 series, the trends were calculated for the periods from 1915 onward.

Schlosser and Oerter [2002b] found that the δ^{18}O record from core B04 was not temperature related since the air temperature record from the nearby Neumayer station did not show a similar trend during the overlapping time period. We will discuss this question in more detail in section 3.3.

[17] Figure 5 shows MTM spectral estimates of the S100 δ^{18}O record calculated using 7 tapers with time-bandwidth set to 4 [see *Thomson*, 1982]. The spectrum has a pronounced "red" character and shows some periodicities that appear as significant at the 95% significance level. For establishing the null hypothesis we assumed that the background (i.e., the original) process can adequately be described by the AR(1) model (autoregressive process of the first order). The analysis identifies a highly significant (above 99% level) variability at a nearly bidecadal scale of 20–25 years, accompanied by a less pronounced peak centered at about 9 years. Several significant peaks at timescales of 2–5 years close to typical ENSO scales are also found. These peaks are, however, not precisely aligned with typical ENSO-scale variations at QB (quasibiannual) and QQ (quasiquadrennial) scale, as demonstrated in Figure 6. The first mode of ENSO variability in SST, as characterized by Niño-3.4 index, shows QQ variations at the shorter scale of about 3.6 years. The second mode manifested in variability in the SST gradient across equatorial Pacific and represented by TNI index show, in turn, QQ variations at a somewhat longer scale of about 4.7 years. At the same time, a shorter SAM index time series was also found to demonstrate the variability at similar timescales of about 2 and 4 years [*Visbeck and Hall*, 2004].

[18] Four of the significant components identified in S100 spectrum represent about 80% of the variability in the original oxygen isotope record. Hereafter we use the naming conventions QBD (quasibidecadal), QD (quasidecadal), QQ (quasiquadrennial) and QB (quasibiannual) following the terminology presented by *Trenberth* [1975], *Jiang et al.* [1995], and *White and Tourre* [2003]. MTM analysis of the B04 core record (Figure 7) reveals similar statistically significant variability at 2.6, 4.1 and 8.2 years. The bidecadal mode is, however, not pronounced.

[19] In order to highlight the variations at different timescales we performed the reconstruction of the oxygen-isotope time series using the periodicities identified by MTM as significant. For convenience, low-frequency (QBD + QD) and high-frequency (QQ + QB) components were calculated separately (see Figure 5). There is evidence for relatively weakened interannual variance in the analyzed series during the end of the 18th and first half of the 19th centuries, which is in line with a decreased amplitude of the ENSO and tropical sea surface temperature (SST) variability during this period [*Mann et al.*, 2000]. The already mentioned well documented period of a weaker ENSO during the 1920s–1950s [*Torrence and Compo*, 1998], however, did not leave a similar imprint in the analyzed record. Still, a decreased variability during this time period was clearly captured in the B04 core.

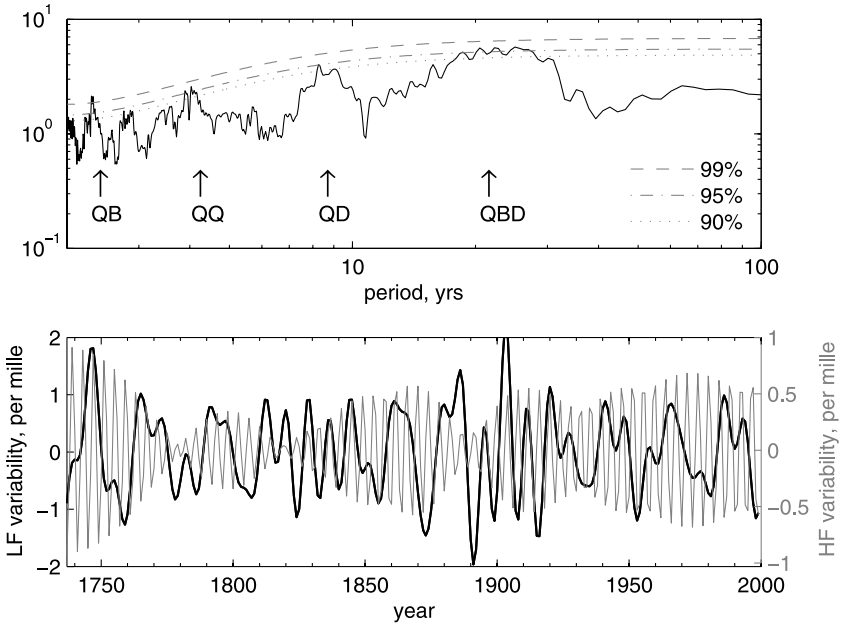

Figure 5. (top) MTM power spectrum of the S100 δ^{18}O time series. Gray dashed, dash-dotted and dotted lines designate 99%, 95%, and 90% significance levels relative to the estimated red noise background. The marks QB, QQ, QD, and QBD designate the quasibiannual, quadrennial, decadal, and bidecadal components, respectively. (bottom) MTM reconstructions of the interannual (QB + QQ) and (bi)decadal (QD + QBD) anomalies of S100 δ^{18}O variability based on significant low- and high-frequency components of the spectral estimate.

3.2. Equatorial Pacific Variability as a Pacemaker for Atmospheric Circulation Changes in the Southern Polar Atlantic

[20] What are the mechanisms and the relative role of ENSO in driving the δ^{18}O variations in the coastal DML ice cores? The studies of *Turner* [2004], *Yuan* [2004], *Mo and Paegle* [2001], and *Fogt and Bromwich* [2006] based on the relatively short series of instrumental data from the subpolar Antarctic proposed the mechanisms linking the tropics and Antarctica. *Gregory and Noone* [2008] recently extended the analysis back in time by examining the effect of ENSO-related circulation changes on oxygen isotope variations in ice cores from West Antarctica.

[21] The strong variability seen in our cores on timescales close to typical ENSO suggests that the driving force can originate in the tropical Pacific. However, a direct comparison with Niño-3.4 index, indicative of SST fluctuations in the Pacific, does not provide an unambiguous answer. Moreover, an inspection of individual ENSO events suggests that positive and negative δ^{18}O anomalies are observed in years with warm as well as cold ENSO events. These results are not unexpected in view of dating errors in combination with the complex nature of processes forming the isotopic signal at the core site, where forcing from the tropics is only one of the players.

[22] Figure 8 shows the wavelet coherence between the annual mean S100 δ^{18}O and Niño-3.4 and TNI indices of ENSO evolution. The analysis demonstrates that all records exhibit coherent variations on the scales above approximately 16 years. The generally warmer SST in the Pacific are positively correlated with S100 isotope record on bidecadal scales and above, as indicated by arrows pointing

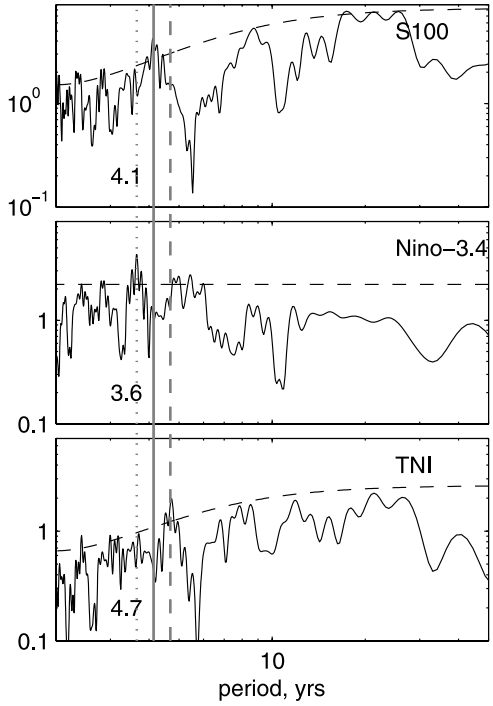

Figure 6. MTM (two tapers, resolution 3) power spectrum of S100 δ^{18}O, September–November (SON) Niño-3.4 and TNI indices of ENSO variability. All three spectra are estimated for the time interval of 1872–1999. The dashed lines designate 90% significance levels relative to the estimated red noise background.

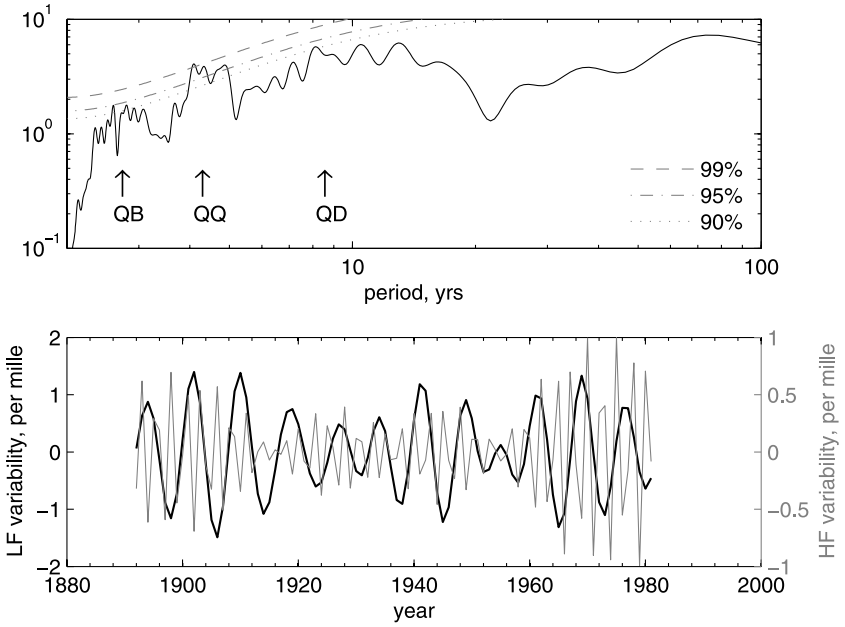

Figure 7. Same as Figure 5, but for core B04.

right in the top panel. The left orientation of the arrows in the bottom panel suggests that higher than the average S100 δ^{18}O are associated with the westward SST gradient in the tropical Pacific (preferentially negative TNI). This also corresponds to a westward displacement in position of the enhanced tropical convection in the equatorial Pacific and the ENSO-driven high (or low) sea level pressure pattern in the Amundsen and Bellingshausen seas [*Bromwich et al.*, 2004]. This relationship, however, does not hold for shorter scales. In particular, during 1900–1930 both indices are in phase at decadal scale and positively correlated with S100 oxygen isotope. On scales less than 4 years only a few patches of statistically significant coherence are revealed in both panels and no robust conclusion about phasing can be reached. The analysis for seasons other than austral spring (September, October, November (SON)) yielded similar results on bidecadal scales.

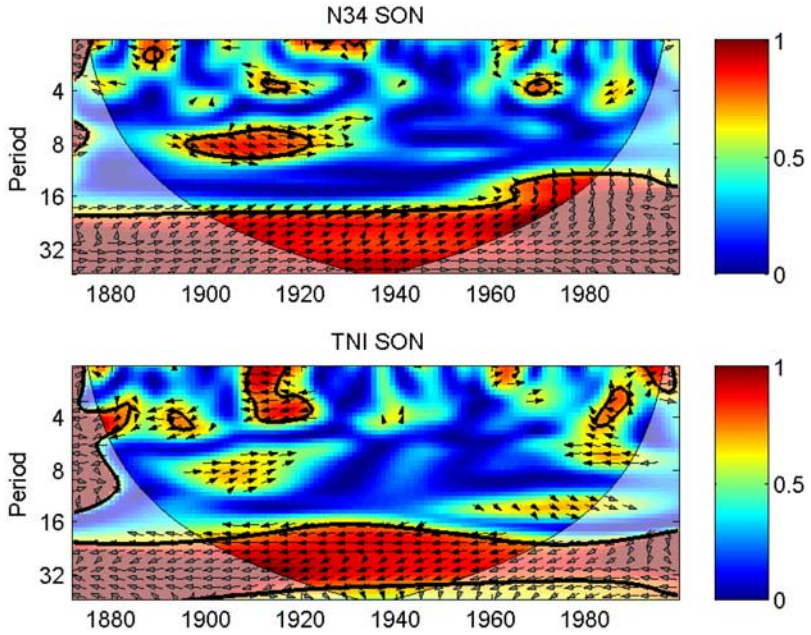

Figure 8. Squared wavelet coherence [*Grinsted et al.*, 2004] between the annual mean S100 δ^{18}O and (top) SON Niño-3.4 and (bottom) TNI indices of ENSO variability. Thick contours enclose the areas with correlations statistically significant at 95% confidence level against red noise. Semitransparent areas indicate the "cone of influence" where the edge effects become important. The relative phase relationship is shown as arrows, with in-phase pointing right and antiphase pointing left.

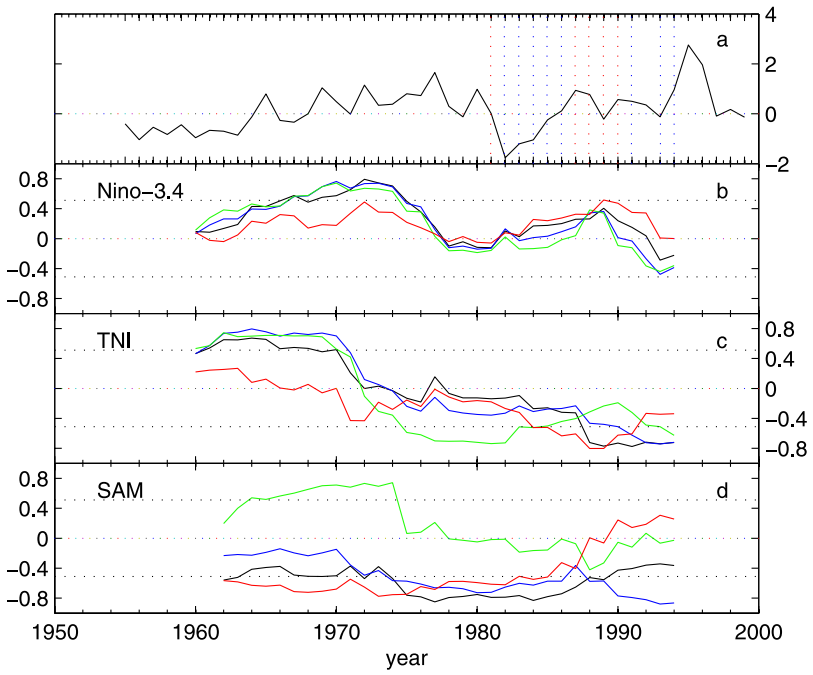

Figure 9. (a) Stacked δ^{18}O anomaly (in nondimensional units) for 1955–1999 for coastal DML obtained from seven ice cores; red and blue dotted vertical lines denote isotopically "warm" and "cold" years, respectively, as was inferred from weekly accumulation measurements from a stake array at Neumeyer during 1981–1996 [see *Schlosser and Oerter*, 2002a, for details]. 10-year running correlation between band-pass filtered in the band 2–8 years stacked coastal δ^{18}O record and band-pass filtered seasonal indices of (b) Niño-3.4, (c) TNI, and (d) SAM. Green, red, black, and blue are used to denote spring (SON), summer (DJF), autumn (MAM), and winter (JJA), respectively. Correlations above (below) 0.51 (−0.51) are statistically significant at the 95% confidence level.

[23] A reliable analysis of the interannual variability in an individual δ^{18}O record is hindered by errors in the core chronology. To rule out, or at least minimize, potential misinterpretation caused by dating errors in a single oxygen isotope series, we constructed a composite record from all available δ^{18}O time series from coastal DML, except Core A. The stacked record (Figure 9a) spans the period 1955–1999. It was produced by averaging the normalized δ^{18}O records from the study area relative to the common period of 1955–1991 (the shorter B04 series was normalized relative to 1955–1980). Panels b, c and d in Figure 9 display running 10-year correlations between the composite record and the seasonal indices of ENSO variability and SAM. In order to focus on shorter timescales, the series of indices as well as the stacked record were band-pass filtered in the band 2–6 years.

[24] Figure 9 demonstrates the uneven effect of ENSO-associated variability on isotopic composition of annual precipitation in coastal DML, in agreement with wavelet coherence results. Seasonal correlations with Niño-3.4 shown in panel b are essentially positive after approximately 1965 and before 1975 and tend to show a less pronounced increase again for the short period centered at 1988. A similar change in sign of the correlation is observed for seasonal TNI (panel c), although it has occurred somewhat earlier than for Niño-3.4.

[25] These results suggest that on the timescales shorter than 6 years during the period before mid 1970s and to a lesser extent in the end of 1980s, the less depleted (isotopically "warm") coastal DML δ^{18}O values were mainly associated with El Niño events and westward SST gradient in the equatorial Pacific. The period in between is characterized by almost zero correlation implying weakened ENSO teleconnection to coastal DML. We note that *Gregory and Noone* [2008] found nearly similar time variation in the relationship between the Southern Oscillation (SOI) index and δ^{18}O from ITASE 2001-5 core to the west of Antarctic Peninsula after the 1960. SOI is indicative of tropical circulation anomalies associated with ENSO-driven SST variations and anticorrelates with Niño-3.4. It implies the presence of the seesaw pattern in oxygen isotope response to ENSO variability between the two areas.

[26] Our results are not in line with *Yuan* [2004], suggesting the negative response in SAT to warm ENSO events to have place in DML area due to the ENSO-driven Antarctic Dipolar Pattern (ADP). However, [*Yuan*, 2004] inference is based on consideration of a relatively short period (after 1980), for which our results do show periods with weak but negative correlations. Of considerable interest is also the timing of the shift from essentially positive to close to zero or slightly negative correlations between seasonal Niño-3.4 and stacked δ^{18}O about 1975. It is coincident with the switch in the evolution of ENSO at the time of 1976/77 [*Trenberth and Stepaniak*, 2001]. Whether these two events are related requires further study.

[27] The correlation with seasonal SAM on the interannual scales seems to be more consistent throughout time (see Figure 9d). With the exception of austral spring, the

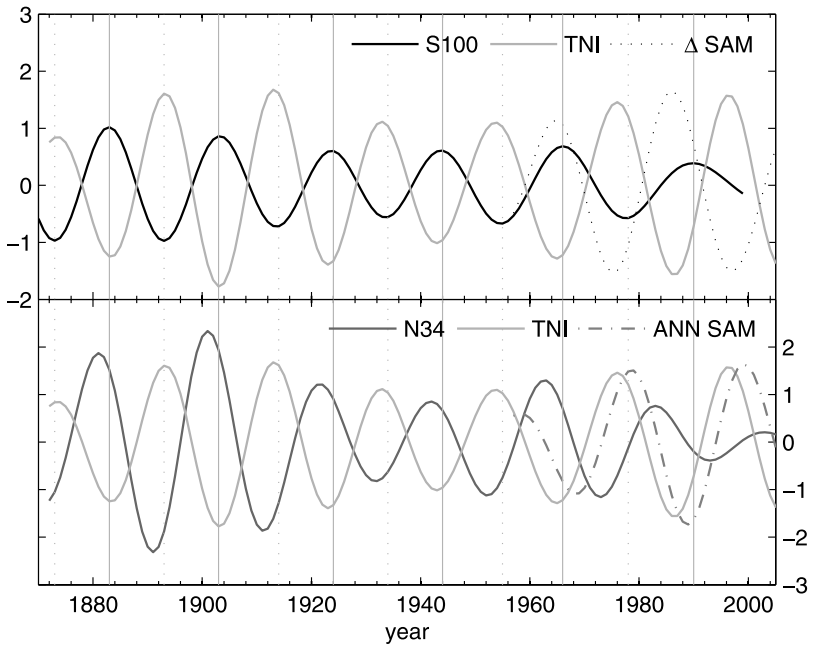

Figure 10. (top) Wavelet band-pass filtered in the band 18–25 years series of annual mean S100 δ^{18}O (black), SON TNI (gray), and normalized spring-summer SAM gradient (dotted gray, see text for details). (bottom) Wavelet band-pass filtered in the band 18–25 years series of SON Niño-3.4 (black), SON TNI (gray), and normalized annual SAM (gray dash-dot) indices. Vertical solid and dashed gray lines in both panels highlight the maxima and minima in S100 δ^{18}O QBD component.

negative coastal DML δ^{18}O anomalies are associated with positive anomalies in SAM. This lies in a general agreement with a conceptual effect of SAM on air temperatures in this part of Antarctica. SAM in the positive phase is associated with decreased polar pressure and strengthened circumpolar westerlies. It induces cooling over most of East Antarctica including the study area [*van den Broeke and van Lipzig*, 2004] implying stronger isotopic depletion [*Noone and Simmonds*, 2002]. Notable is that an opposite relationship between SAM and δ^{18}O during the 1960s–1980s has emerged from the analysis of *Gregory and Noone* [2008] for ice cores from West Antarctica. This is broadly in line with the SAM-driven seesaw in SAT between the part of West (mainly Antarctic Peninsula) and East Antarctica. Note that the largest magnitudes of correlations between seasonal SAM indices (all except SON) and stacked DML δ^{18}O are observed during approximately 1975–1985. This is also a period of a weaker teleconnection from the tropics, as evidenced by nearly zero correlations of δ^{18}O with seasonal Niño-3.4 indices (Figure 9b). These results points to a prevalence of the SAM influence on isotopic composition of accumulation in the study area during this decade. Noteworthy is the opposite trends in correlations between winter and summer, toward a more significant role of winter SAM and less significant role of summer SAM throughout the period covered by the composite record. This is suggestive of a change in response to seasonal forcing on isotopes in the study area.

[28] In contrast to interannual to subdecadal scale variations, variations at longer scales demonstrate high coherence with ENSO indices that is consistent through time. We note that the coherence of this QBD variations in S100 δ^{18}O and Niño-3.4 again is not consistent with the expected negative response to warm ENSO events, as depicted in [*Yuan*, 2004].

[29] In order to isolate the QBD variations in the analyzed records we filtered the records in the band 18–25 years. Figure 10 displays a distinct antiphase relationship between S100-δ^{18}O and TNI. The agreement between the records is not so good for the last 20 years of data, which can be due to both dating errors (see section 3.1) and edge effects of band-pass filtering procedure. At the same time, the positive correlation between the oxygen isotope series and Niño-3.4 is less stable. It suggest that not only the sign of the ENSO event (“warm” or “cold”, or actually the epoch of preferentially positive or negative ENSO events), but rather their configuration will have an effect on the isotopic signature of the annual accumulation. We therefore incline to ascribe the presence of QBD variations to forcing from the second mode of ENSO variability represented by TNI. However, the actual mechanism propagating the signal from the tropics and shaping the oxygen isotope record is yet to be defined.

[30] Brevity of the available instrumental records from Antarctica does not allow us to unambiguously assign a cause to the pronounced bidecadal variations in S100 δ^{18}O. The presence of variations at this timescale was previously reported for sea salt records from the Law Dome and Siple Dome ice cores [*Goodwin et al.*, 2004; *Kreutz et al.*, 2000] as well as from MSA records from the Weddell Sea area [*Abram et al.*, 2007]. As a potential driving mechanism the long-term variations in the strength of SAM were proposed.

[31] *Fogt and Bromwich* [2006] identified the decadal scale changes in the strength of ENSO teleconnections to Antarctica, specifically during the austral spring. A stronger signature of ENSO-driven circulation changes in the south-

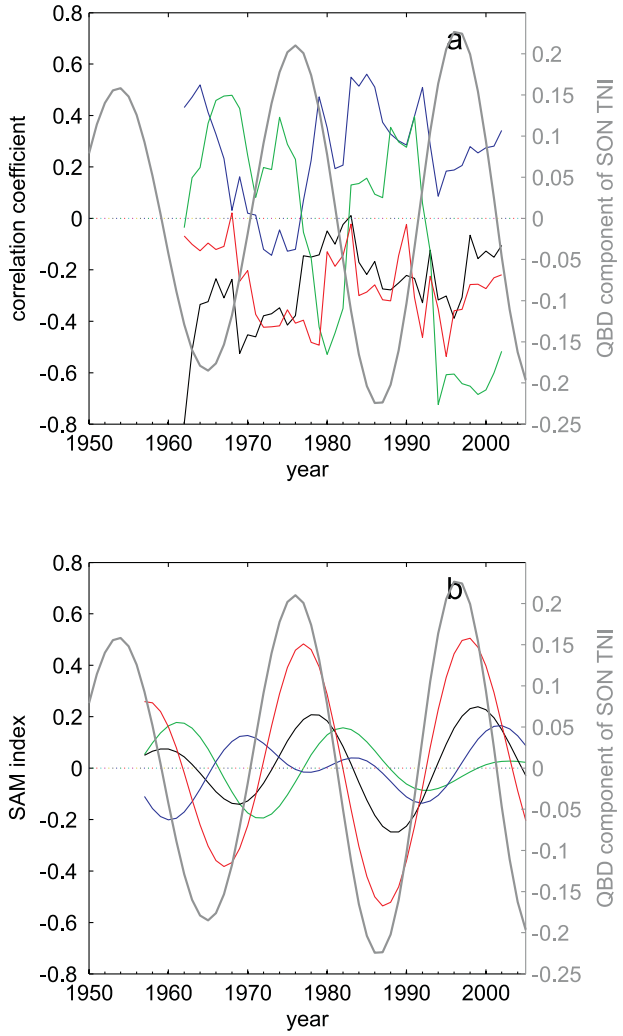

Figure 11. (a, left axis) 10-year running correlation between SON (green), DJF (red), MAM (black), and JJA (blue) Niño-3.4 and SAM indices; (right axis) wavelet band-pass filtered in the band 18–25 years SON TNI (gray). (b, left axis) Wavelet band-pass filtered in the band 18–25 years seasonal SAM indices; the color convention is the same as in Figure 11a; (right axis) same as in Figure 11a.

eastern Pacific and southwestern Atlantic during the 1990s compared with 1980s were ascribed to SON SOI and SAM being in phase (i.e., Niño-3.4 and SAM in antiphase). We extended this analysis back to 1957 and to the other seasons. Figure 11 shows 10-year running correlations between seasonal Niño-3.4 and SAM indices. For SON the correlations tend to alternate between positive and negative values on the decadal scale, in agreement with conclusions of *Fogt and Bromwich* [2006]. The other seasons, especially December, January, February (DJF), also demonstrate variability in coupling between SOI and SAM at decadal scales, which is, however, less pronounced than for SON. The latter is not unusual as austral spring and summer are supposed to best capture ENSO's influence on Antarctica since it is during these seasons that ENSO events are in their mature stage.

[32] The bottom panel in Figure 11 demonstrates the band-pass filtered series of seasonal SAM indices for the period of 1957–2007 shown together with the filtered TNI index. The plot reveals almost synchronous, with a lag of few years, variability in bidecadal DJF SAM and TNI. Austral spring and autumn SAM lag the TNI variations, whereas for winter the phasing is unclear. The resulting annual mean SAM (Figure 10) lags the TNI by 3–4 years indicating that increase in TNI is generally associated with intensification of westerlies around Antarctica, as indicated by the increasing SAM.

[33] We hypothesize that the role of TNI-driven variability in the Pacific SST can be related with longitudinal shifts in position of the maximum of tropical convection and hence the Rossby wave train, which forms in response to warm and cold ENSO events. It, in turn, affects the position of ENSO teleconnection pattern in the southeast Pacific. Since the major loading center of the SAM pattern is located in the area of the Amundsen and Bellingshausen seas [e.g., *Thompson and Wallace*, 2000], a better alignment with the ENSO-driven high(low) pressure center during El Niño (La Niña) in this area will promote more negative (positive) SAM. This is consistent with *L'Heureux and Thompson* [2006] who found, though for the shorter timescales, that La Niña events tend to enhance the westerlies at approximately 60°S, which is equivalent to increasing the SAM index. As however suggested *Harangozo* [2004], the ENSO modulation of the southeast Pacific exratropical circulation also depends on the spatial configuration of the tropical convection. We note from Figure 11 that increase in the strength of ENSO teleconnection coincides with the periods of lasting positive QBD TNI. During the 1970s and 1990s, a stronger (anti)correlation between (Niño-3.4) SOI and SAM, which is specific for spring and summer seasons, promotes thereby strengthening of SON, DJF and MAM SAM (see bottom panel in Figure 10). The opposite is observed in the 1960s and 1980s.

[34] The effect of SAM variability on isotopic composition of accumulated snow has a complex nature. The net effect of bidecadal variations in SAM on δ^{18}O S100 is conditioned by a relative phasing of variations in the seasonal SAM, a seasonal asymmetry in SAT and δ^{18}O response to SAM variations [*Marshall*, 2007] as well as potential bias in seasonal accumulation. Following the analysis presented by *Schlosser* [1999] and *Schlosser and Oerter* [2002b], increase in spring and decrease in summer SAM modifies the accumulation seasonality leading to more isotopically "cold" spring and "warm" summer snow in the annual accumulation. This decreases the mean δ^{18}O in the annual accumulation. The smoothed interseasonal spring to summer SAM gradient, which we define as the difference between SON and DJF SAM index, is in antiphase with the smoothed ENSO TNI, i.e., in phase with S100 δ^{18}O. This result is consistent with what was found for the shorter timescales but actually opposite to the conclusions of *Schlosser* [1999] and *Schlosser and Oerter* [2002b]. It yet does not contradict them as their findings stem from the 15-yearlong series of observations and show an integrated effect of variations at all timescales and processes including those not considered in the present study. The positive and negative δ^{18}O anomalies in the

stacked record also not always coincide with isotopically "cold" and "warm" years as was identified by *Schlosser and Oerter* [2002b] (see also in Figure 9). Since the more positive (negative) SAM in the study area is generally associated with cooling (warming [*van den Broeke and van Lipzig*, 2004; *Hall and Visbeck*, 2002]) which promotes isotopic depletion (enrichment [*Noone and Simmonds*, 2002]), our results suggest that on bidecadal scales the thermal effect on S100 δ^{18}O overrides the possible effect of seasonal SAM fluctuations on accumulation seasonality. It also corroborates the hypothesis of [*Abram et al.*, 2007] which linked the bidecadal variability in methanesulfonic acid (MSA) in three coastal ice cores from the Weddel Sea area with the strength of cold offshore wind anomalies, a mechanism associated with the long term changes in the state of SAM. Note that extrema in a smoothed interseasonal SAM gradient match well the maxima in the amplitude of semiannual oscillation (SAO [*van den Broeke*, 1998]), a semiannual mode of variability in position of the circumpolar trough [*van Loon*, 1967; *van den Broeke*, 1998], which is closely related to SAM. It indicates that the actual effect of SAO strength on QBD variations in S100 isotopes depends on the relative signs of seasonal SAM.

[35] It is clear that the shortness of SAM record as well as the edge effects of the band-pass filtering questions a robustness of this hypothesis. However, the stability of the inferred antiphase relationship between QBD TNI and S100 δ^{18}O throughout more than 100 years of instrumental data on SST suggests that ENSO variations do affect the long-term variations in annual isotopic composition of snow accumulation via modulation of SAM. The assessment of a relative contribution of temperature variability and accumulation seasonality changes to δ^{18}O variations on these scales requires a better understanding of the mechanisms of interactions between SAM, ENSO and local climate. Both longer instrumental series, including *in situ* accumulation measurements, and/or relevant regional modeling studies would be helpful.

3.3. To the Source of Trends in δ^{18}O in the Coastal DML

[36] Based on model outputs, precipitation increases are often suggested to be an indicator of warming in polar regions [e.g., *Huybrechts et al.*, 2004]. In line with the pronounced warming observed in the Arctic in the last decades, the warming process is anticipated to take place in the Antarctic as well. The shortness of available instrumental data, however, hinders us from reaching any unambiguous conclusions about spatiotemporal patterns of changes in atmospheric temperatures [*Turner et al.*, 2005, 2006] and accumulation [*Monaghan et al.*, 2006] in Antarctica. We therefore find it important to also view available ice core records from the area, specifically the longer δ^{18}O and accumulation records of S100 and B04 (Figure 2). The accumulation record of ice core S100 suggests a decrease since 1900 when it had some of the highest accumulation values since the 1730s [*Kaczmarska et al.*, 2004]. Decreasing trend in accumulation has also been reported from other, shallower cores from the same coastal area [*Isaksson and Melvold*, 2002, and references therein] including those considered in the present work. The four more recent ice cores B39(1935–2006), B38, FB0704 and FB0702(1960–2006) retrieved from the area to the south of Neumayer do demonstrate increasing annual δ^{18}O but do not reveal any common pattern in accumulation [*Oerter et al.*, 2008]. We note that these cores were drilled on the ridges Halvfarryggen and Søråsen where the effects of enhanced wind erosion compared with the other locations considered should not be ruled out. Notable is that the composite accumulation record from 16 cores retrieved on the higher altitude DML plateau exhibits an opposite (increasing) trend in accumulation and weak positive trend in δ^{18}O during the 20th century [*Graf et al.*, 2002]. No persistent secular scale changes in accumulation since 1900 are seen in H72 core from eastern DML [*Nishio et al.*, 2002]. Two Berkner Island cores R1 and B25, in turn, show increase from around 1920 (R1) or no clear trend (B25) in accumulation, and increase in δ^{18}O since 1950s [*Mulvaney et al.*, 2002]. It suggests therefore that this overall picture of a positive trend in δ^{18}O and a negative in accumulation is a regional signal [*Kaczmarska et al.*, 2004] likely confined to low elevations in western coastal DML.

[37] One should note that assessment and interpretation of trends in stable isotopes in the study area is not straightforward. The presence of pronounced variations on decadal scales and longer, potential for changes in seasonality of accumulation, stratigraphic noise as well as variations in moisture transport and sources, condition a high sensitivity of the estimated trend to a time interval selected. This effect is illustrated in Figure 12 showing the calculated trends in the instrumental SAT and the equivalent temperature trends estimated from the isotope records and their first principal component. The analysis uses the instrumental data from the two nearest meteorological stations that have sufficiently long temperature records: Novolazareveskaya (started in 1961) and Halley (started in 1957). The trends were estimated for the periods of overlap between the ice core and instrumental series. For conversion between δ^{18}O and T we applied a local estimate of δ-T gradient of 0.53‰ K^{-1}, based on 19 years (1981–2000) of *in situ* measurements from Neumayer station [*Schlosser et al.*, 2004].

[38] Figure 12 demonstrates that the estimates of trends in isotopic records vary substantially depending on the time period as well as the location considered. The scatter in the trends in the annual mean SAT is correspondingly less pronounced. Except for the core S20 showing the trend at least twice as steep compared with the other isotope records, the trend magnitudes are generally confined to the interval [0,0.8] K dec^{-1} and close, within an error interval, to correspondent trends in SAT. Note that the magnitudes of trends are higher, on average, for the period of overlap with a longer Halley temperature record due to a period of successive years with decreased δ^{18}O values in the end of the 1950s. A systematic positive offset between the trends in isotopes and SAT, though not yet exceeding the uncertainty, is also evident for Halley where surface air temperatures tend to show a weak cooling during the last five decades [*Turner et al.*, 2005].

[39] We note that the trends estimated for longer δ^{18}O records from S100 and B04, as well as for core E (Figure 4) are essentially positive and similar in magnitudes to the trend found in PC1. Since no substantial disagreement in trends is found either between the shorter SAT and δ^{18}O records, this can be interpreted as an indication of a long term warming that begun in this part of DML as early as in

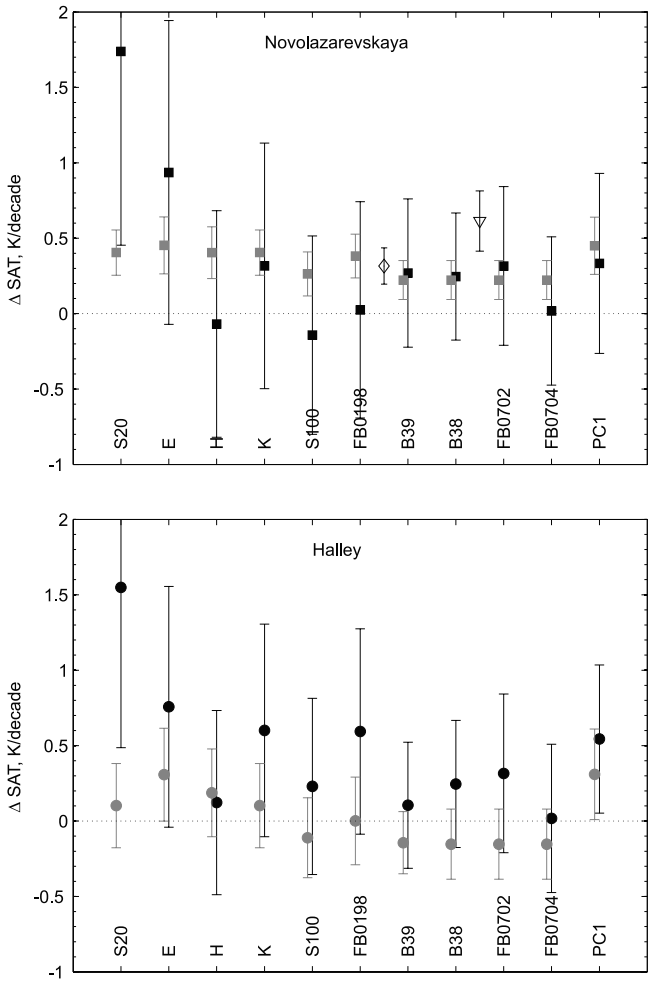

Figure 12. Linear trends in δ^{18}O in the ice cores from coastal DML converted into equivalent trends in SAT (black solid squares and circles). The time periods used to calculate the trend magnitudes overlap with the periods of available instrumental mean annual SAT from (top) Novolazarevskaya (shown by gray solid squares) and (bottom) Halley (gray solid squares). PC1 denotes the first principal component of six δ^{18}O series (see text for details). Open diamond and triangle at the top show the equivalent SAT trends in S100 (1920–1999) and B04 (1920–1981) cores.

the 1910s. This hypothesis is in line with other presumable evidences of early Antarctic warming [e.g., *Schneider et al.*, 2006; *Schneider and Steig*, 2008; *Murphy et al.*, 1995] and a mean warming of the Southern Hemisphere throughout the 20th century [*Jones and Moberg*, 2003].

[40] One still should not discard other processes that could contribute to the secular positive trend annual δ^{18}O in the study area. The coastal areas are known to receive precipitation formed of moisture originating largely from the local sources. Decrease of winter sea ice extent will therefore promote shorter moisture transport paths, implying less distillation en route [*Noone and Simmonds*, 2004]. Available evidences of winter sea ice decline in the subpolar Atlantic throughout the 20th century [*Murphy et al.*, 1995] suggest that this mechanism can potentially contribute to the positive trend in the observed δ^{18}O.

[41] The seasonal redistribution in snow accumulation depicted in [*Schlosser*, 1999; *Schlosser and Oerter*, 2002a] introduces a bias in the annual mean δ^{18}O. This effect was shown to be responsible for a relatively poor correlation of the oxygen isotope records with SAT series from the neighboring weather stations. However, longer than present 14 years long data series is needed in order to reliably assess the potential contribution of this effect to the observed multidecadal positive trends in δ^{18}O records from coastal DML.

4. Conclusions

[42] We used a network of eight ice cores from coastal DML in order to examine the role of ENSO in the temporal variability of δ^{18}O. Despite the substantial spatial extent of the core network, of about 500 km, our analysis reveals that they share a common signal even on interannual timescales. Dating errors as well as the stratigraphic noise in an individual record may pose a substantial limitation on the validity of the inferences made for the shorter timescales. We therefore used the longest S100 ice core record spanning the period of 1737–1999 for analysis only on decadal scales and longer. The shorter stacked coastal DML δ^{18}O series spanning 1955–1999 was constructed to assess the variability of ENSO teleconnection on interannual scales.

[43] The complex nature of the processes driving the isotopic signal in precipitation and the ice cores from DML has already been highlighted in a number of studies [*Schlosser*, 1999; *Schlosser and Oerter*, 2002a, 2002b; *Helsen et al.*, 2006]. The dominance of variability at close to ENSO timescales of 2–6 (Niño-3.4, TNI), 9 and 20–25 (TNI) years in the annual mean δ^{18}O from coastal DML cores points to an important role of the tropics in modulating its local climate. However, as our analysis demonstrated, the response to ENSO variability is not stable in time. Moreover, it also varies depending on the timescale considered as well as the mutual state of SAM and ENSO.

[44] Our results suggest that on typical ENSO timescales of 2–6 years there is no consistent relationship between the stacked DML δ^{18}O and the Niño-3.4 and TNI indices of ENSO evolution. For Niño-3.4 the correlation changes from essentially positive during 1965–1975 to less certain in the most recent part of the record. The TNI index is in phase with δ^{18}O before approximately 1970 and antiphase after 1990. The magnitude of correlation also varies differently for different seasons. This is generally in line with the time varying response to ENSO-associated circulation anomalies demonstrated in *Gregory and Noone* [2008] for the ice core oxygen isotope records from West Antarctica.

[45] The SAM index for all seasons except austral spring shows a more consistent antiphase relationship with DML δ^{18}O. This result agrees well with the general tendency for positive (negative) SAM anomalies to be associated with atmospheric cooling (warming), thereby promoting isotopic depletion (enrichment). This led us to conclude that on these scales the SAM/temperature influence dominates the isotope variability. However, the opposite trends in correlations between the winter and summer, toward a more significant role of winter SAM after 1985, are suggestive of a recent change in response to seasonal forcing on isotopes in the study area.

[46] The clear linkage between ENSO variability and S100 $\delta^{18}O$ appears on the scale of approximately two decades. We found that positive isotope anomalies are associated with periods of oceanic warming (i.e., preferentially positive Niño-3.4) and westward sea surface temperature gradient (i.e., preferentially negative TNI) in the equatorial Pacific. As the positive correlation between the oxygen isotope series and Niño-3.4 is less stable, we conclude that not only the sign of ENSO events (or actually the periods with preferentially warm or cold ENSO events), but rather their configuration will have an effect on the isotopic signature of the annual accumulation at the quasi-bidecadal scale.

[47] We propose the bidecadal scale variability in the strength of SAM forced from the tropics to be a critical element in the teleconnection between the tropical Pacific and coastal DML at longer timescales. In line with *Fogt and Bromwich* [2006], our analysis reveals decadal scale variations in the strength of the coupling between the seasonal SAM and Niño-3.4 (SOI). Although this effect seems to be most pronounced for austral spring, similar variations in the magnitude of the correlation are observed for austral summer and autumn. When SOI and SAM are in phase (Niño-3.4 and SAM in antiphase), it causes the SAM to increase, promoting cooling and isotopic depletion in precipitation. The nearly decadal periods of a stronger coupling between SOI and SAM are associated with preferentially positive TNI index, indicative of the eastward shift in the position of the maximum of tropical convection and hence the Rossby wave train, which forms in response to warm and cold ENSO events. The scale of the variations suggests that the ocean is involved in creating and sustaining the persistent SST and atmospheric circulation anomalies in southeast Pacific and subpolar Atlantic, in analogy with the Pacific Decadal Oscillation phenomenon observed in the North Pacific [*Bond and Harrison*, 2000]. We would like to leave this issue, however, beyond the scope of this article.

[48] Our analysis suggests that a multidecadal positive trend of the order of 0.12‰/dec in the annual mean $\delta^{18}O$ values from the analyzed cores may be associated with the atmospheric warming that begun in this part of the DML already in the 1910s. However, in an almost 300-yearlong S100 oxygen isotope series, the $\delta^{18}O$ values during the most recent 50-year period do not show, on average, any more positive $\delta^{18}O$ values than the earliest part of the record, i.e., the mid 1700s. We quantified the trend in $\delta^{18}O$ in terms of long-term surface air temperature (SAT) changes using the empirical $\delta^{18}O/T$ relationship derived for the study area. The trend magnitudes show consistency with the instrumental data. Yet we speculate that the role of other processes not necessarily linearly related with long-term SAT changes like isotopic enrichment due to shrinking winter sea ice should not be underestimated. The source of the negative accumulation trend however remains obscure as it does not fit the observations in the other parts of Antarctica neither supported by modeling.

[49] Our knowledge of Antarctic climate and the role ENSO plays in it is still incomplete. Ice cores provide a variety of information about past climate variations, both on local and global scales, that can be used to improve our understanding of ENSO's effect on Antarctic climate. A better quantification of the physical mechanisms forming the isotopic signal in the ice cores has, however, direct implications for ice core-based reconstruction of climate variability in the past.

[50] **Acknowledgments.** Financial support came from The Norwegian Research Council and EU EPICA-MIS. This work is a Norwegian contribution to International Trans Antarctic Scientific Expedition (ITASE) and the European Project for Ice Coring in Antarctica (EPICA), a joint European Science Foundation/European Commission scientific programme, funded by the EU and by national contributions from Belgium, Denmark, France, Germany, Italy, Netherlands, Norway, Sweden, Switzerland, and the United Kingdom. The main logistic support was provided by IPEV and PNRA (at Dome C) and AWI (at Dronning Maud Land). This is EPICA publication 224. The authors thank three anonymous reviewers for their constructive comments.

References

Abram, N. J., R. Mulvaney, E. W. Wolff, and M. Mudelsee (2007), Ice core records as sea ice proxies: An evaluation from the Weddell Sea region of Antarctica, *J. Geophys. Res.*, *112*, D15101, doi:10.1029/2006JD008139.

Ashok, K., S. K. Behera, S. A. Rao, H. Weng, and T. Yamagata (2007), El Niño Modoki and its possible teleconnection, *J. Geophys. Res.*, *112*, C11007, doi:10.1029/2006JC003798.

Bond, N. A., and D. E. Harrison (2000), The Pacific Decadal Oscillation, air-sea interaction and central North Pacific winter atmospheric regimes, *Geophys. Res. Lett.*, *27*, 731–734.

Bromwich, D. H., R. L. Monaghan, and Z. Guo (2004), Modeling the ENSO modulation of antarctic climate in the late 1990s with the polar MM5, *J. Clim.*, *17*, 109–132.

Chaudhuri, P., and J. Marron (1999), SiZer for exploration of structures in curves, *J. Am. Stat. Assoc.*, *94*, 807–823.

EPICA Community Members (2006), One-to-one coupling of glacial climate variability in Greenland and Antarctica, *Nature*, *444*(9), 195–198.

Fogt, R. L., and D. H. Bromwich (2006), Decadal variability of the ENSO teleconnection to the high-latitude south Pacific governed by coupling with the southern annular mode, *J. Clim.*, *19*, 979–997, doi:10.1175/JCLI3671.1.

Ghil, M., et al. (2002), Advanced spectral methods for climatic time series, *Rev. Geophys.*, *40*(1), 1003, doi:10.1029/2000RG000092.

Godtliebsen, F., L. R. Olsen, and J.-G. Winther (2003), Recent developments in statistical time series analysis: Examples of use in climate research, *Geophys. Res. Lett.*, *30*(12), 1654, doi:10.1029/2003GL017229.

Goodwin, I. D., T. D. van Ommen, M. A. J. Curran, and P. A. Mayewski (2004), Mid latitude winter climate variability in the South Indian and southwest Pacific regions since 1300 AD, *Clim. Dyn.*, *22*, 783–794, doi:10.1007/s00382-004-0403-3.

Graf, W., H. Oerter, O. Reinwarth, W. Stichler, F. Wilhelms, H. Miller, and R. Mulvaney (2002), Stable-isotope records from Dronning Maud Land, Antarctica, *Ann. Glaciol.*, *35*, 195–201.

Gregory, S., and D. Noone (2008), Variability in the teleconnection between the El Niño–Southern Oscillation and West Antarctic climate deduced from West Antarctic ice core isotope records, *J. Geophys. Res.*, *113*, D17110, doi:10.1029/2007JD009107.

Grinsted, A., J. Moore, and S. Jevrejeva (2004), Application of the cross wavelet transform and wavelet coherence to geophysical time series, *Nonlinear Proc. Geophys.*, *11*, 561–566.

Hall, A., and M. Visbeck (2002), Synchronous variability in the Southern Hemisphere atmosphere, sea ice, and ocean resulting from the annular mode, *J. Clim.*, *15*, 3043–3057, doi:10.1175/1520-0442(2002)015.

Harangozo, S. A. (2004), The relationship of Pacific deep tropical convection to the winter and springtime extratropical atmospheric circulation of the South Pacific in El Niño events, *Geophys. Res. Lett.*, *31*, L05206, doi:10.1029/2003GL018667.

Helsen, M. M., R. S. W. van de Wal, M. R. van den Broeke, V. Masson-Delmotte, H. A. J. Meijer, M. P. Scheele, and M. Werner (2006), Modeling the isotopic composition of Antarctic snow using backward trajectories: Simulation of snow pit records, *J. Geophys. Res.*, *111*, D15109, doi:10.1029/2005JD006524.

Huybrechts, P., J. Gregory, I. Janssens, and M. Wild (2004), Modelling Antarctic and Greenland volume changes during the 20th and 21st centuries forced by GCM time slice integrations, *Global Planet. Change*, *42*, 83–105.

Isaksson, E., and W. Karlén (1994), Spatial and temporal patterns in snow accumulation, western Dronning Maud Land, Antarctica, *J. Glaciol.*, *40*, 399–409.

Isaksson, E., and K. Melvold (2002), Trends and patterns in the recent accumulation and oxygen isotopes in coastal Dronning Maud Land, Antarctica: Interpretations from shallow ice cores, *Ann. Glaciol.*, *35*, 175–180.

Isaksson, E., W. Karlén, N. Gundestrup, P. Mayewski, S. Whitlow, and M. Twickler (1996), A century of accumulation and temperature changes in Dronning Maud Land, Antarctica, *J. Geophys. Res.*, *101*, 7085–7094.

Isaksson, E., M. R. van den Broeke, J.-G. Winther, L. Karlöf, J. F. Pinglot, and N. Gundestrup (1999), Accumulation and proxy-temperature variability in Dronning Maud Land, Antarctica, determined from shallow firn cores, *Ann. Glaciol.*, *29*, 17–22.

Jiang, N., J. D. Neelin, and M. Ghil (1995), Quasi-quadrennial and quasi-biennial variability in the equatorial Pacific, *Clim. Dyn.*, *12*, 101–112.

Jones, P. D. (1990), Antarctic temperatures over the present century—a study of the early expedition record, *J. Clim.*, *3*, 1193–1203.

Jones, P. D., and A. Moberg (2003), Hemispheric and large-scale surface air temperature variations: An extensive revision and an update to 2001, *J. Clim.*, *16*, 206–223, doi:10.1175/1520-0442(2003)016.

Kaczmarska, M., et al. (2004), Accumulation variability derived from an ice core from coastal Dronning Maud Land, Antarctica, *Ann. Glaciol.*, *39*, 339–345.

Kaczmarska, M., E. Isaksson, L. Karlof, O. Brandt, J.-G. Winther, R. van de Wal, M. van den Broeke, and S. Johnsen (2006), Ice core melt features in relation to Antarctic coastal climate, *Antarct. Sci.*, *18*, 271–278.

King, J. C., and S. A. Harangozo (1998), Climate change in the western Antarctic Peninsula since 1945: Observations and possible causes, *Ann. Glaciol.*, *27*, 571–575.

Kreutz, K. J., P. A. Mayewski, I. I. Pittalwala, L. D. Meeker, M. S. Twickler, and S. I. Whitlow (2000), Sea level pressure variability in the Amundsen Sea region inferred from a West Antarctic glaciochemical record, *J. Geophys. Res.*, *105*, 4047–4060.

L'Heureux, M. L., and D. W. J. Thompson (2006), Observed relationships between the El Niño Southern Oscillation and the Extratropical Zonal-Mean Circulation, *J. Clim.*, *19*, 276–287, doi:10.1175/JCLI3617.1.

Mann, M., R. Bradley, and M. Hughes (2000), Long-term variability in the El Nino Southern Oscillation and associated teleconnections, in *El Nino and the Southern Oscillation: Multiscale Variability and Its Impacts on Natural Ecosystems and Society*, edited by H. Diaz and V. Markgraf, 512 pp., Cambridge Univ. Press, Cambridge, U. K.

Marshall, G. J. (2003), Trends in the Southern annular mode from observations and reanalyses., *J. Clim.*, *16*, 4134–4143.

Marshall, G. J. (2007), Half-century seasonal relationships between the Southern Annular mode and Antarctic temperatures, *Int. J. Climatol.*, *27*, 373–383, doi:10.1002/joc.1407.

Melvold, K. (1999), Impact of recent climate on glacier mass balance: Studies on Kongsvegen, Svalbard and Jutulstraumen, Antarctica, Ph.D. thesis, Univ. of Oslo, Oslo, Norway.

Mo, K. C., and J. N. Paegle (2001), The Pacific-South American modes and their downstream effects, *Int. J. Climatol.*, *21*, 1211–1229.

Monaghan, A. J., et al. (2006), Insignificant change in Antarctic snowfall since the International Geophysical Year, *Science*, *313*, 827–831, doi:10.1126/science.1128243.

Mulvaney, R., H. Oerter, D. A. Peel, W. Graf, C. Arrowsmith, E. C. Pasteur, B. Knight, G. C. Littot, and W. D. Miners (2002), 1000 year ice-core records from Berkner Island, Antarctica, *Ann. Glaciol.*, *35*, 45–51.

Murphy, E., A. Clarke, C. Symon, and J. Priddle (1995), Temporal variation in Antarctic sea-ice: Analysis of a long term fast-ice record from the South Orkney Islands, *Deep-Sea Res. I*, *42*(7), 1045–1062.

Nishio, F., et al. (2002), Annual-layer determinations and 167 year records of past climate of H72 ice core in east Dronning Maud Land, Antarctica, *Ann. Glaciol.*, *35*, 471–479.

Noone, D., and I. Simmonds (2002), Annular variations in moisture transport mechanisms and the abundance of δ^{18}O in Antarctic snow, *J. Geophys. Res.*, *107*(D24), 4742, doi:10.1029/2002JD002262.

Noone, D., and I. Simmonds (2004), Sea ice control of water isotope transport to Antarctica and implications for ice core interpretation, *J. Geophys. Res.*, *109*, D07105, doi:10.1029/2003JD004228.

Oerter, H., F. Fernandoy, H. Meyer, F. Wilhelms, W. Graf, and W. Stichler (2008), Accumulation and stable-isotope content in the hinterland of Neumayer station, Antarctica, since the IGY 1957/58, in *XXX SCAR Open Science Meeting, 10–13 July*, St. Petersburg, Russia.

Parkinson, C. (2004), Southern Ocean sea ice and its wider linkages: Insights revealed from models and observations, *Antarct. Sci.*, *16*, 387–400, doi:10.1017/S0954102004002214.

Percival, D., and A. Walden (2000), *Wavelet Methods for Time Series Analysis*, 620 pp., Cambridge Univ. Press, Cambridge, U.K.

Schlosser, E. (1999), Effects of seasonal variability of accumulation on yearly mean δ^{18}O values in Antarctic snow, *J. Glaciol.*, *45*, 463–468.

Schlosser, E., and H. Oerter (2002a), Seasonal variations of accumulation and the isotope record in ice cores: A study with surface snow samples and firn cores from Neumayer station, Antarctica, *Ann. Glaciol.*, *35*, 97–101.

Schlosser, E., and H. Oerter (2002b), Shallow firn cores from Neumayer, Ekströmisen, Antarctica: A comparison of accumulation rates and stable-isotope ratios, *Ann. Glaciol.*, *35*, 91–96.

Schlosser, E., C. H. Reijmer, H. Oerter, and W. Graf (2004), The influence of origin of precipitation on the d^{18}O-T relationship at Neumayer station, Ekströmisen, Antarctica, *Ann. Glaciol.*, *39*, 41–48.

Schneider, D., and E. Steig (2008), Ice cores record significant 1940s Antarctic warmth related to tropical climate variability, *Proc. Natl. Acad. Sci.*, *105*(34), 12,154–12,158, doi:10.1073/pnas.0803627105.

Schneider, D. P., E. J. Steig, T. D. van Ommen, D. A. Dixon, P. A. Mayewski, J. M. Jones, and C. M. Bitz (2006), Antarctic temperatures over the past two centuries from ice cores, *Geophys. Res. Lett.*, *33*, L16707, doi:10.1029/2006GL027057.

Thompson, D. W. J., and J. M. Wallace (2000), Annular modes in the extratropical circulation: Part I. Month-to-month variability, *J. Clim.*, *13*, 1000–1016, doi:10.1175/1520-0442(2000)013.

Thomson, D. (1982), Spectrum estimation and harmonic analysis, *Proc. IEEE*, *70*, 1055–1096.

Torrence, C., and G. Compo (1998), A practical guide to wavelet analysis, *Bull. Am. Meteorol. Soc.*, *79*(1), 61–78.

Trenberth, K. E. (1975), A quasi-biennial standing wave in the Southern Hemisphere and interrelations with sea surface temperature, *Q. J. R. Meteorol. Soc.*, *101*, 55–74.

Trenberth, K. E., and D. P. Stepaniak (2001), LETTERS: Indices of El Niño Evolution, *J. Clim.*, *14*, 1697–1701.

Turner, J. (2004), Review—the El Nino-Southern Oscillation and Antarctica, *Int. J. Climatol.*, *24*, 1–31.

Turner, J., S. R. Colwell, G. J. Marshall, T. A. Lachlan-Cope, A. M. Carleton, P. D. Jones, V. Lagun, P. A. Reid, and S. Iagovkina (2005), Antarctic climate change during the last 50 years, *Int. J. Climatol.*, *25*, 279–294.

Turner, J., T. A. Lachlan-Cope, S. Colwell, G. J. Marshall, and W. M. Connolley (2006), Significant warming of the Antarctic winter troposphere, *Science*, *311*, 1914–1917, doi:10.1126/science.1121652.

van den Broeke, M. (1998), The semi-annual oscillation and Antarctic climate: Part 2. Recent changes, *Antarct. Sci.*, *2*, 184–191.

van den Broeke, M. R., and N. P. M. van Lipzig (2004), Changes in Antarctic temperature, wind and precipitation in response to the Antarctic Oscillation, *Ann. Glaciol.*, *39*, 119–126.

van Loon, H. (1967), The half-yearly oscillations in middle and high southern latitudes and the coreless winter, *J. Atmos. Sci.*, *24*, 472–486.

Vaughan, D., and C. Doake (1996), Recent atmospheric warming and retreat of ice shelves on the Antarctic Peninsula, *Nature*, *379*, 328–331, doi:10.1038/379328a0.

Visbeck, M., and A. Hall (2004), Comments on "Synchronous variability in the southern hemisphere atmosphere, sea ice, and ocean resulting from the annular mode"—Reply, *J. Clim.*, *17*, 2255–2258, doi:10.1175/1520-0442(2004)017.

White, W., and R. Peterson (1996), An Antarctic circumpolar wave in surface pressure, wind, temperature and sea ice extent, *Nature*, *380*, 699–702.

White, W. B., and Y. M. Tourre (2003), Global SST/SLP waves during the 20th century, *Geophys. Res. Lett.*, *30*(12), 1651, doi:10.1029/2003GL017055.

Yuan, X. (2004), ENSO-related impacts on Antarctic sea ice: A synthesis of phenomenon and mechanisms, *Antarc. Sci.*, *16*, 415–425.

D. V. Divine, E. Isaksson, and M. Kaczmarska, Norwegian Polar Institute, Polar Environmental Centre, N-9296 Tromsø, Norway. (dmitry.divine@npolar.no; elli@npolar.no)

F. Godtliebsen, Department of Mathematics and Statistics, University of Tromsø, N-9037 Tromsø, Norway.

S. J. Johnsen, Centre for Ice and Climate, Niels Bohr Institute, University of Copenhagen, Juliane Maries Vej 30, DK-2100 Copenhagen OE, Denmark.

H. Oerter, Alfred Wegener Institute for Polar and Marine Research, Am Alten Hafen 26, Building D-3330, D-27568 Bremerhaven, Germany.

E. Schlosser, Institute of Meteorology and Geophysics, University of Innsbruck, Innrain 52, A-6020 Innsbruck, Austria.

R. S. W. van de Wal and M. van den Broeke, Institute for Marine and Atmospheric Research, Utrecht University, P.O. Box 80005, 3508TA Utrecht, Netherlands.